Title

Cerebral perfusion in posterior reversible encephalopathy syndrome measured with arterial spin labeling MRI

Journal

NeuroImage Clinical, 35(J. Magn. Reson. Imaging 43 1 2016)

ISSN

2213-1582

Authors

Fazeli, Soudabeh
Noorbakhsh, Abraham
Imbesi, Steven G
et al.

Publication Date

2022

DOI

10.1016/j.nicl.2022.103017

Peer reviewed

NeuroImage: Clinical 35 (2022) 103017

Contents lists available at ScienceDirect

NeuroImage: Clinical

journal homepage: www.elsevier.com/locate/ynicl

Cerebral perfusion in posterior reversible encephalopathy syndrome measured with arterial spin labeling MRI

Soudabeh Fazeli [a], Abraham Noorbakhsh [a], Steven G. Imbesi [a], Divya S. Bolar [a,b,*]

[a] Department of Radiology, University of California San Diego, 200 W. Arbor Drive, San Diego, CA 92103, United States
[b] Center for Functional Magnetic Resonance Imaging, University of California San Diego, 9500 Gilman Drive, La Jolla, CA 92093, United States

ARTICLE INFO

Keywords:
Posterior reversible encephalopathy syndrome
Cerebral blood flow
Arterial spin labeling
ASL
PRES
CBF

ABSTRACT

Background and purpose: The pathophysiologic basis of posterior reversible encephalopathy syndrome (PRES) remains controversial. Hypertension (HTN)-induced autoregulatory failure with subsequent hyperperfusion is the leading hypothesis, whereas alternative theories suggest vasoconstriction-induced hypoperfusion as the underlying mechanism. Studies using contrast-based CT and MR perfusion imaging have yielded contradictory results supporting both ideas. This work represents one of the first applications of arterial spin labeling (ASL) to evaluate cerebral blood flow (CBF) changes in PRES.

Materials and methods: After obtaining Institutional Review Board approval, MRI reports at our institution from 07/2015 to 09/2020 were retrospectively searched and reviewed for mention of "PRES" and "posterior reversible encephalopathy syndrome." Of the resulting 103 MRIs (performed on GE 1.5 Tesla or 3 Tesla scanners), 20 MRIs in 18 patients who met the inclusion criteria of clinical and imaging diagnosis of PRES and had diagnostic-quality pseudocontinuous ASL scans were included. Patients with a more likely alternative diagnosis, technically non-diagnostic ASL, or other intracranial abnormalities limiting assessment of underlying PRES features were excluded. Perfusion in FLAIR-affected brain regions was qualitatively assessed using ASL and characterized as hyperperfusion, normal, or hypoperfusion. Additional quantitative analysis was performed by measuring average gray matter CBF in abnormal versus normal brain regions.

Results: HTN was the most common PRES etiology (65%). ASL showed hyperperfusion in 13 cases and normal perfusion in 7 cases. A hypoperfusion pattern was not identified. Quantitative analysis of gray matter CBF among patients with visually apparent hyperperfusion showed statistically higher perfusion in affected versus normal appearing brain regions (median CBF 100.4 ml/100 g-min vs. 61.0 ml/ 100 g-min, $p < 0.001$).

Conclusion: Elevated ASL CBF was seen in the majority (65%) of patients with PRES, favoring the autoregulatory failure hypothesis as a predominant mechanism. Our data support ASL as a practical way to assess and non-invasively monitor cerebral perfusion in PRES that could potentially alter management strategies.

1. Introduction

Posterior reversible encephalopathy syndrome (PRES) is a potentially reversible neurotoxic state typically associated with a distinctive pattern of symmetrically distributed brain vasogenic edema on CT and MRI (Bartynski, 2008; Hinchey et al., 1996; Casey et al., 2000). The parieto-occipital regions are most commonly affected followed by the posterior frontal and temporal lobes and the cerebellum (Bartynski, 2008; Casey et al., 2000). Hypertension (HTN) is the most commonly identified etiology of PRES, but it has also been recognized in the setting of a number of medications and systemic conditions, such as high dose immunosuppressive or cytotoxic medications, preeclampsia/eclampsia, impaired renal function, autoimmune diseases, malignancy, sepsis, and shock (Bartynski, 2008; Casey et al., 2000; Fischer and Schmutzhard, 2017). Clinical presentation typically includes seizures, headache, altered mental status, or visual symptoms (Bartynski, 2008; Hinchey et al., 1996).

Although PRES is a well-recognized neurological disorder for almost three decades (Hinchey et al., 1996), its pathophysiology remains controversial (Fischer and Schmutzhard, 2017; Bartynski, 2008). HTN-

Abbreviations: CBF, Cerebral blood perfusion; PRES, Posterior reversible encephalopathy syndrome; HTN, Hypertension; ASL, Arterial spin labeling; MAP, Mean arterial pressure; AMS, Altered mental status.

* Corresponding author at: UCSD Center for Functional Magnetic Resonance Imaging, 9500 Gilman Drive MC 0677, La Jolla, CA 92093, United States.
E-mail address: dbolar@ucsd.edu (D.S. Bolar).

https://doi.org/10.1016/j.nicl.2022.103017
Received 12 January 2022; Received in revised form 12 March 2022; Accepted 22 April 2022
Available online 30 April 2022

induced autoregulatory failure with subsequent hyperperfusion is currently the leading hypothesis (Fischer and Schmutzhard, 2017; Bartynski, 2008; Schwartz et al., 1995). According to this theory, severe hypertension exceeding the upper limits of CBF autoregulation (~150 mmHg) results in cerebral arterial hyperperfusion and subsequent blood brain barrier (BBB) breakdown and vasogenic edema (Fischer and Schmutzhard, 2017; Bartynski, 2008). A related alternative theory suggests that extreme HTN results in vasoconstriction and hypoperfusion, with subsequent local ischemia, BBB breakdown, and vasogenic edema (Bartynski, 2008; Anderson et al., 2020). Arguing against HTN-induced failed autoregulation/dysregulation theories is that blood pressure is normal to only mildly elevated in about one-third of patients with PRES (Fischer and Schmutzhard, 2017; Feske, 2011). As such, a second theory proposes endothelial dysfunction caused by circulating endogenous or exogenous toxins as the underlying mechanism of PRES (Fischer and Schmutzhard, 2017; Bartynski, 2008; Marra et al., 2014). With this theory, vasoconstrictive and immunogenic agents released by damaged vascular endothelial cells are thought to mediate vasospasm and/or increased BBB permeability, leading to cerebral hypoperfusion and edema formation (Bartynski, 2008; Anderson et al., 2020; Marra et al., 2014).

Prior studies using contrast-enhanced MR and CT perfusion imaging and Tc99m-hexamethylpropyleneamine oxime (Tc99m-HMPAO) SPECT have yielded contradictory results (Bartynski, 2008; Schwartz et al., 1995; Apollon et al., 2000; Hedna et al., 2012; Wartenberg and Parra, 2006; Vanacker et al., 2015; Sarbu et al., 2014). While a number of early case reports and series have reported hyperperfusion in the setting of PRES (Schwartz et al., 1995; Apollon et al., 2000; Hedna et al., 2012; Wartenberg and Parra, 2006), more recent studies have shown reduced CBF in affected regions (Vanacker et al., 2015; Sarbu et al., 2014). Improved understanding of CBF changes in the setting of PRES may help better elucidate the underlying etiology and potentially inform management strategies.

Arterial spin labeling (ASL) allows noninvasive quantitative assessment of CBF without intravenous contrast (Alsop et al., 2015) and provides a practical way to assess perfusion in PRES. To our knowledge, only a single published abstract has used ASL to assess perfusion changes in a small group of patients with PRES (Whitlow et al., 2008). Therefore, the aim of this study was to evaluate CBF changes in a larger series of PRES patients using ASL.

2. Materials and methods

2.1. Subject selection and data collection

The study was approved by the Institutional Review Board. Given the retrospective and observational nature of the study, the need for patient consent was waived.

ASL was incorporated into routine clinical brain MR protocols at our institution in July 2015. A search of all reports from MRIs performed at our institution between July 2015 to September 2020 was conducted, using inclusion search terms of "PRES" and "posterior reversible encephalopathy syndrome". Of the resulting 103 MR reports with the above search terms, 20 MRIs in 18 patients were included in the final analysis. The inclusion criteria were confirmed clinical and imaging diagnosis of PRES and available diagnostic-quality ASL scans. These studies were identified and included in the final analysis. The diagnosis of PRES was established based on characteristic patterns of brain vasogenic edema on FLAIR sequences along with typical PRES symptoms (as determined by the clinical team). The exclusion criteria were unlikely diagnosis of PRES based on clinical and/or imaging findings, presence of a more likely alternative clinical or imaging diagnosis (e.g. infarct, infection, etc.), presence of other intracranial abnormalities (e.g. diffuse metastatic disease) limiting assessment of underlying PRES, or absent or technically non-diagnostic ASL. The study population flow diagram is presented in Fig. 1.

Demographic and clinical data including clinical presentation, physiological and laboratory data, and PRES etiology were extracted from the patients' electronic medical records (Table 1).

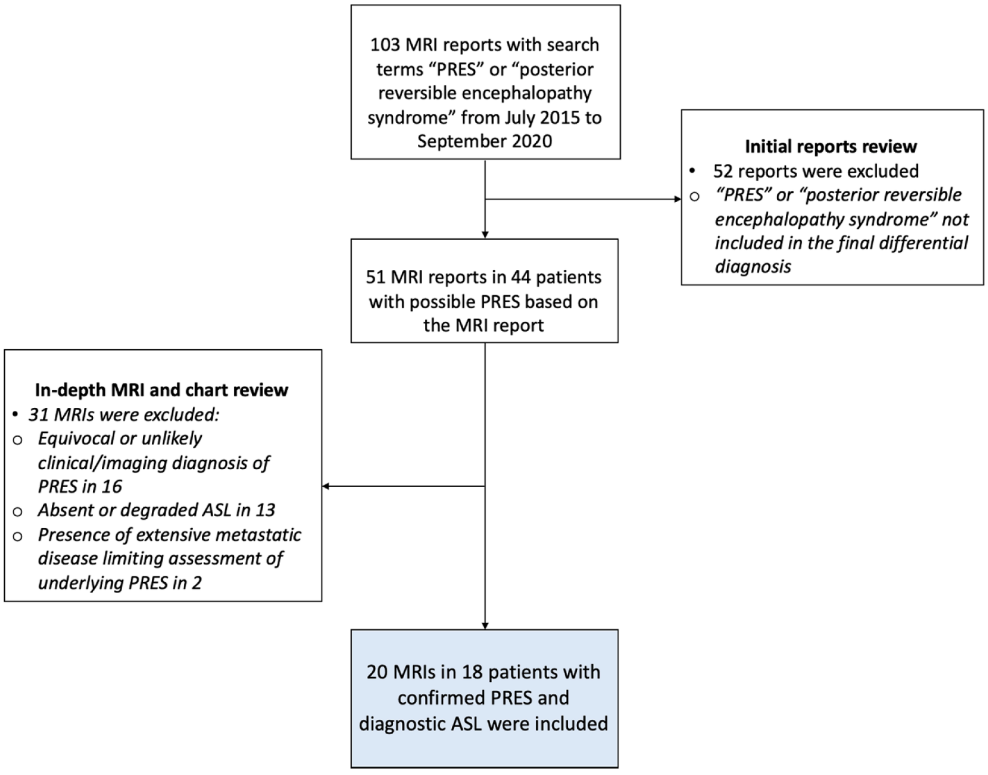

Fig. 1. Study flow diagram.

Table 1
Summary of clinical and imaging data for each individual patient with final diagnosis of PRES.

Patient #	Age	Gender	Clinical presentation	MAP	PRES etiology	Time from symptoms onset to imaging (days)	Affected brain regions	ASL perfusion	Restricted diffusion	Microhemorrhage	PRES outcome[1]
1	53	Female	Seizure, headache, vision change	90	Renal insufficiency	1	Parieto-occipital, frontal	Hyperperfusion	No	No	Favorable
2	36	Male	Dysarthria and disequilibrium	146	HTN	6	Brainstem	Normal[2]	No	No	Favorable
3	21	Female	Seizure, headache, vision change	114	HTN	0	Parieto-occipital	Hyperperfusion	No	No	Favorable
	21	Female	Seizure, headache, vision change	170	HTN	1	Parieto-occipital, frontal, temporal, cerebellum	Hyperperfusion	Yes	Yes	Favorable
4	24	Female	Seizure	116	HTN	3	Frontal, parieto-temporal, cerebellum	Normal	Yes	Yes	Unfavorable[3]
5	33	Male	Seizure, headache	107	Methamphetamine	0	Parieto-occipital, frontal	Hyperperfusion	Yes	Yes	Favorable
	33	Male	Seizure, headache	78	Methamphetamine	3	Parieto-occipital	Normal	Yes	Yes	Favorable
6	73	Female	AMS, headache	129	Bevacizumab	1	Frontal, occipital, temporal, cerebellum, thalami, brainstem	Hyperperfusion	Yes	Yes	Unfavorable[4]
7	58	Female	Bilateral upper extremity weakness	78	Oxaliplatin/ Capecitabine	15	Parieto-occipital, frontal, cerebellum	Hyperperfusion	Yes	No	Unfavorable[5]
8	47	Male	Right facial droop, vision change	152	HTN	0	Parieto-occipital, frontal	Hyperperfusion	No	No	Favorable
9	23	Female	Seizure, vision change	164	HTN	0	Parieto-occipital	Hyperperfusion	No	No	Favorable
10	17	Female	Seizure, headache	123	HTN[6]	0	Parieto-occipital, frontal, temporal	Normal	No	No	Favorable
11	47	Male	AMS, seizure	92	Methamphetamine	3	Parietal, frontal, cerebellum	Normal	Yes	No	Favorable
12	63	Female	AMS, seizure		HTN	1	Parieto-occipital, frontal	Hyperperfusion	No	Yes	Favorable
13	59	Male	Seizure	148	HTN	1	Parieto-occipital, frontal, temporal	Hyperperfusion	No	Yes	Favorable
14	62	Female	AMS	135	HTN	1	Parieto-occipital, frontal	Hyperperfusion	No	No	Favorable
15	63	Male	Seizure	162	HTN	0	Parieto-occipital, frontal, cerebellum, basal ganglia, thalami	Hyperperfusion	No	No	Favorable
16	60	Male	AMS, seizure	100	Sirolimus	2	Occipital	Normal	No	No	Unfavorable[7]
17	56	Female	AMS	112	HTN	0	Brainstem, parietal	Hyperperfusion	No	Yes	Favorable[8]
18	74	Male	AMS	145	HTN	0	Parieto-occipital, cerebellum	Normal	No	No	Favorable

[1] Based on resolution of clinical symptoms of PRES versus presence or absence of long standing clinical or imaging sequela, and evolution of imaging findings on follow up MRI.
[2] Perfusion was difficult to assess on ASL given the brainstem location.
[3] Patient developed right lower extremity weakness secondary to brainstem lacunar infarcts.
[4] Patient developed left upper extremity weakness with no follow-up imaging available.
[5] Patient developed bilateral upper extremity weakness with no follow-up imaging available.
[6] In the setting of eclampsia.
[7] Patient developed worsening PRES and pontine infarct and ultimately succumbed.
[8] Patient recovered from PRES but ultimately succumbed secondary to graft versus host disease.
Note: Case 3 had two brain MRIs obtained during two distinct episodes of PRES (with complete interval resolution). Case 5 had two brain MRIs obtained during the same episode of PRES.
MAP, mean arteria pressure; PRES, posterior reversible encephalopathy syndrome; ASL, arterial spin labeling; AMS, altered mental status; HTN, hypertension.

2.2. Imaging technique

MRI examinations were performed on either a GE Signa 1.5 Tesla or 3 Telsa scanner (GE Healthcare, Milwaukee, Wisconsin). All MRI studies included T2-weighted, T2 FLAIR, DWI, SWI and ASL sequences.

ASL was performed with the GE product pseudocontinuous ASL (pCASL) sequence (General Electric, Milwaukee, WI), which incorporates a 3D stack-of-spirals fast spin echo readout. pCASL-specific parameters include a labeling duration of 1.5 s and post labeling delay (PLD) of 2 s (adapted from ASL white paper recommendations (Alsop et al., 2015). 3D spiral readout parameters include spiral interleaves = 8, points per spiral = 512, slices = 36, in-plane resolution: 3.64–4.53 mm^2, slice thickness = 4.0 – 4.2 mm, FOV = 24–26 cm, TE = 9.5–10.5 ms, bandwidth = 62.5 kHz, TR = 4800–4847 ms, NEX = 3, and scan time = 4 m 32 s to 4 m 42 s.

2.3. Imaging analysis and assessment of cerebral perfusion

MRI examinations were blindly and independently reviewed by a neuroradiology fellow (four years radiology experience) and an attending neuroradiologist (eight years radiology experience). Vasogenic edema in affected brain regions was identified based on FLAIR/T2 signal abnormalities. Cerebral perfusion in patients with FLAIR abnormality was qualitatively assessed using ASL and characterized as hyperperfusion, normoperfusion, or hypoperfusion. Of note, the readers were careful to not count ASL signal residing in the macrovasculature (so-called arterial transit artifact, ATA) as true hyperperfusion (See Discussion). In patients with visually apparent abnormal cerebral perfusion (hyper- or hypoperfusion), additional quantitative CBF analysis was performed. Specifically, ROIs were drawn to encompass areas of abnormal gray matter CBF (either hyper or hypo) as identified on ASL imaging. An ROI tool was used to first draw an outline around contiguous voxels with visually apparent abnormal perfusion. This was done on a slice-by-slice basis, independent of the FLAIR abnormality. To serve as a control, CBF was also measured by drawing an ROI in a normal-appearing region on contiguous slices. Specifically, if the CBF abnormality was unilateral, the control ROI was drawn in the contralateral gray matter. If the CBF abnormality was bilateral or in the brainstem, anterior frontal regions were used for comparison (which typically contained normally perfused areas). A large control ROI of at least 20 ml (>1200 voxels) was used to improve accuracy of the control CBF estimate.

Additional relevant MRI features including which brain region(s) were affected, presence or absence of restricted diffusion, and presence or absence of hemorrhage were also assessed and documented. Follow up imaging (if available) was also reviewed to identify any irreversible sequalae (e.g. infarct).

2.4. Statistical analysis

The primary outcomes of the study included qualitative ASL perfusion (hyperperfusion vs. normoperfusion vs. hypoperfusion) and quantitative CBF (ml/100 g-min) in the affected versus normal brain regions among patients with qualitatively abnormal brain perfusion.

Independent demographic, clinical, and imaging covariates included age, gender, mean arterial pressure (MAP), PRES etiology, number of days between initial clinical presentation and the MRI exam, presence of restricted diffusion or hemorrhage, and clinical outcome. Given the small sample size, PRES etiology was dichotomized into HTN (the most common etiology) vs. other etiologies for bivariate analyses. Similarly, the number of days between initial clinical presentation and MRI exam (time to imaging) was dichotomized into “24 h or less” and “ more than 24 h”.

Association between qualitative ASL perfusion (i.e.., hyper, normal, or hypo) and demographic, clinical, and imaging correlates were examined using the Fisher’s exact test for categorical variables and Wilcoxon Rank Sum test for continuous variables.

Wilcoxon Signed Rank test was used to compare quantitative ASL CBF in the affected versus normal brain regions. Inter-reader agreement was assessed using Fleiss kappa statistics. All statistical analyses were performed using R, Version 4.0.2.

3. Results

3.1. Sample characteristics

The demographic, clinical, and imaging data for each individual patient with a confirmed clinical and imaging diagnosis of PRES is summarized in Table 1. In the 20 included MRIs, the median age was 50.1 (range 17–74, interquartile range (IQR) 32.8–59.7) and 9 (45%) were males. The median for mean arterial pressure (MAP) was 123 (range 78–170, IQR 107–147). The most common presenting signs and symptoms were seizure (n = 13), altered mental status (n = 7), headache (n = 7), and vision changes (n = 5). HTN was the most common reported etiology (n = 13), followed by medications/drugs (n = 6), and renal insufficiency (n = 1).

3.2. Imaging findings and cerebral perfusion on ASL

Time interval between initial clinical presentation and brain MRI (time to imaging) was 24 h or less in 14 cases and greater than 24 h in 6 cases. Conventional MR images demonstrated typical findings of PRES with both symmetrically and asymmetrically distributed vasogenic edema predominantly involving the cerebral cortex and subcortical white matter, as well as to a lesser degree the cerebellum, brain stem, and deep gray nuclei. The parieto-occipital regions (n = 19) were the most commonly involved, followed by the frontal lobe (n = 13) and cerebellum (n = 7). In one patient, only the brainstem was involved (central-variant PRES McKinney et al., 2013). Foci of restricted diffusion and microhemorrhages were observed in seven and eight patients, respectively. Imaging findings for each individual patient are also summarized in Table 1.

ASL showed hyperperfusion (Fig. 2) in 13 (65%) and normal perfusion (Fig. 3) in 7 (35%) patients. Of those patients with HTN-induced PRES (n = 13), 69% demonstrated hyperperfusion (n = 9). Assessment of perfusion had excellent agreement between readers with Fleiss kappa of 0.88 (95%CI = 0.68–1.00). The single case with initial disagreement was reviewed and discussed by the readers together to reach a consensus.

CBF changes were often seen to spatially correlate with FLAIR abnormality, although this was not always the case. The extent of ASL abnormality was similar in size to FLAIR hyperintensity in 5 patients (matched scenario), larger than FLAIR hyperintensity in 5 patients, and smaller than FLAIR hyperintensity in 9 patients (unmatched scenarios); in one patient, there were distinct areas of ASL abnormality without FLAIR hyperintensity and areas of FLAIR hyperintensity without ASL abnormality (unmatched scenario). Fig. 4 shows representative examples of both matched and unmatched ASL and FLAIR abnormality.

Short interval follow-up brain MRI was available in one patient who had a brain MRI at the time of initial presentation and a repeat exam during the same admission for PRES. CBF changes (hyperperfusion) were initially observed corresponding to the regions of FLAIR signal abnormality; however, they near-completely resolved on the follow-up MRI performed 3 days later. In contrast, FLAIR signal abnormality was stable without improvement on follow-up (Fig. 5). The other patient who had a repeat MRI presented with new symptoms over two months after the initial symptoms resolved; as such, these data were treated as distinct presentations.

Quantitative assessment of gray matter CBF in areas of apparent elevated perfusion on ASL showed statistically significant elevated CBF (median = 100.4 ml/min, interquartile range = 88.9 – 115.4) relative to regions of normally perfused (control) brain (median = 61.0 ml/min,

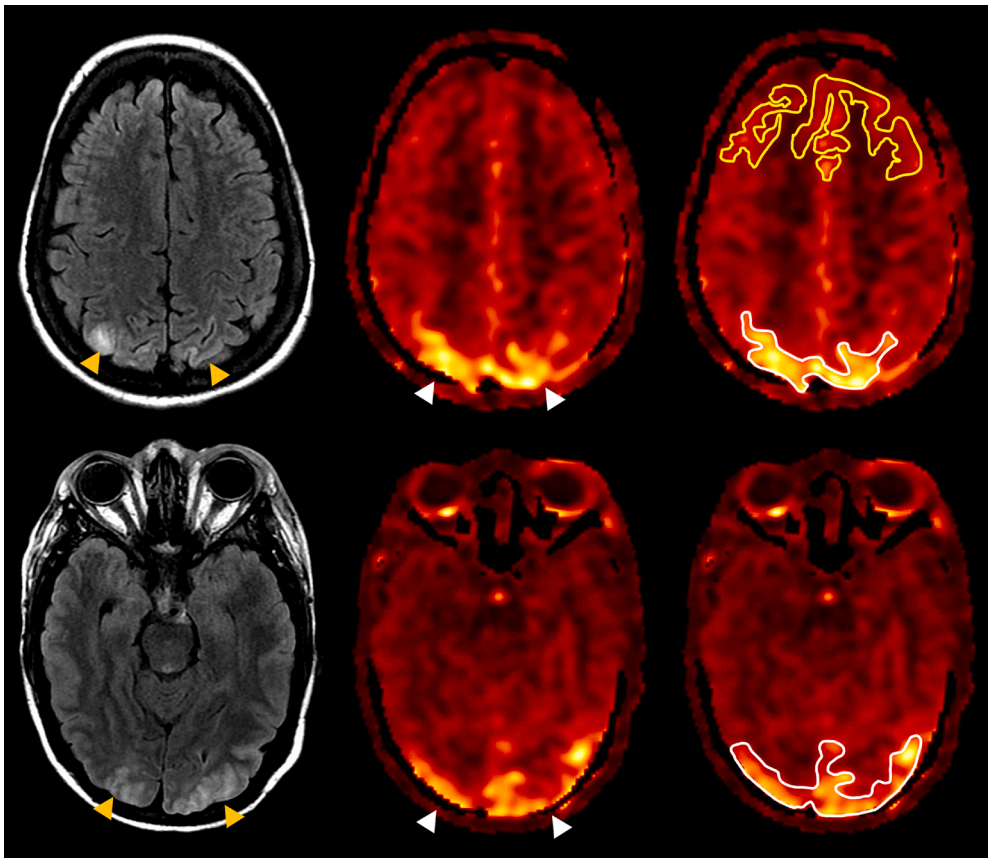

Fig. 2. Axial T2 FLAIR (left) and ASL perfusion maps (middle and right) in a 23-year-old female with Tacrolimus-induced PRES. Hyperperfusion (white arrowheads) is noted corresponding to the regions of parieto-occipital FLAIR hyperintensity (yellow arrowheads). Regions-of-interest (ROI) are depicted for hyperperfusion (white outline) and normal perfusion (yellow outline). Note that ROIs extend into adjacent slices (not shown). (For interpretation of the references to color in this figure legend, the reader is referred to the web version of this article.)

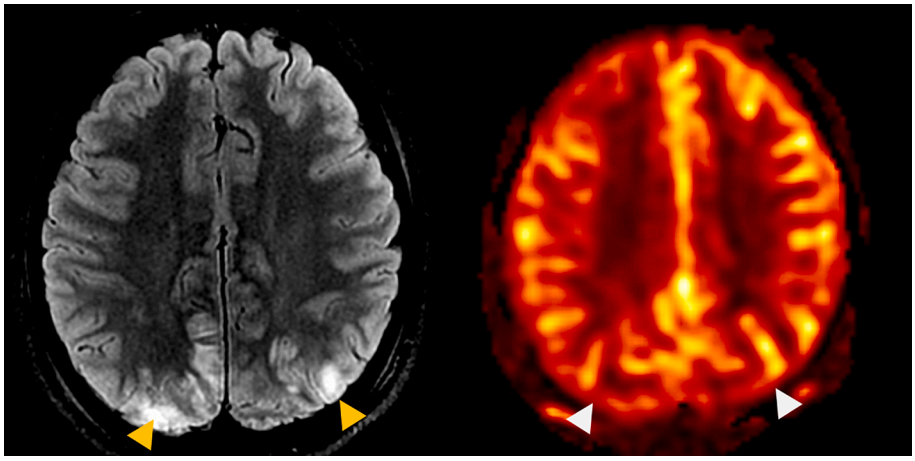

Fig. 3. Axial T2 FLAIR (left) and ASL color (right) perfusion maps in an 18-year-old female with eclampsia induced PRES. No convincing altered perfusion was seen on ASL corresponding to the regions of FLAIR hyperintensity (yellow arrowheads) or elsewhere. (For interpretation of the references to color in this figure legend, the reader is referred to the web version of this article.)

interquartile range = 53.5 – 68.4, $p < 0.001$) (Fig. 6). Mean volume of the hyperperfused regions was 43.5 +/- 47.5 ml, the largest measuring 58.7 ml and smallest measuring 5.5 ml.

Bivariate analyses revealed a statistically significant association between qualitative ASL perfusion assessment and time to imaging; specifically, patients who were imaged in $\leq$ 24 h from initial clinical presentation were more likely to have hyperperfusion on ASL compared to those who were imaged in > 24 h (85.7% vs. 16.7%, $p = 0.007$). No statistically significant associations were found between the remaining demographic, clinical, and imaging covariates and qualitative ASL perfusion (Table 2). In addition, no statistically significant association was found between ASL/FLAIR signal abnormality mismatch and time to imaging.

4. Discussion

Our study represents one of the first applications of ASL to assess cerebral perfusion changes in PRES and found hyperperfusion as the predominant pattern among our sample of twenty PRES cases. Three important observations were made: 1) hyperperfusion was seen in nearly two-thirds of the patients, favoring the HTN-induced autoregulatory failure hypothesis as a dominant mechanism; 2)

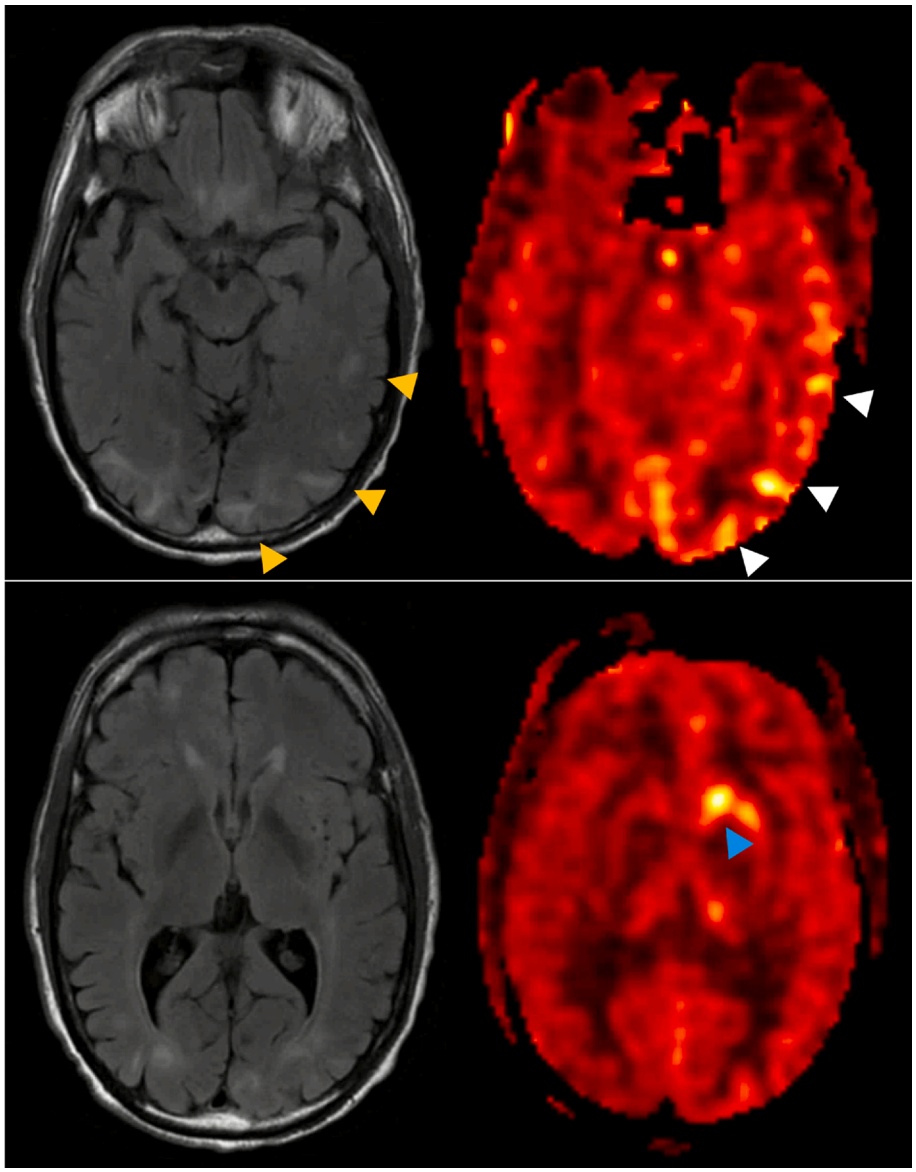

Fig. 4. A representative example of both matched and unmatched ASL and FLAIR abnormality. Axial T2 FLAIR (left) and ASL color (right) perfusion maps in a 59-year-old male with HTN-induced PRES. Hyperperfusion (white arrowheads) is noted corresponding to the regions of FLAIR hyperintensity (orange arrowheads). Hyperperfusion without any corresponding FLAIR hyperintensity is seen in the left basal ganglia (blue arrowhead). (For interpretation of the references to color in this figure legend, the reader is referred to the web version of this article.)

hyperperfusion was most likely to be present in patients imaged less than 24 h from symptom onset, and 3) quantitative assessment of gray matter CBF among hyperperfusion patients showed an average of ~65% increase in CBF in areas of elevated perfusion relative to normally perfused brain regions (significant at $p < 0.001$). The remaining one-third of patients did not have any apparent cerebral perfusion changes. Importantly, a hypoperfusion pattern was not identified in any of the patients.

Our findings add another set of observations to the already heterogeneous reports of perfusion imaging in PRES, and to our knowledge, this is the largest of these studies, as well as the only study (outside of a conference proceeding) to use ASL for perfusion evaluation. While some studies have reported increased perfusion on CT perfusion (Hedna et al., 2012), MR perfusion (Schwartz, 2002), and SPECT imaging (Schwartz, 2002; Schwartz et al., 1992), other studies using CT (Vanacker et al., 2015; Sarbu et al., 2014; Sanelli et al., 2005) and MR perfusion imaging (Bartynski and Boardman, 2008; Brubaker et al., 2005; Engelter et al., 1999) have reported hypoperfusion as the dominant pattern. For example, Hedna et al. (2012) described increased CBF, CBV, and reduced TTP in the posterior cerebral artery distribution by CT perfusion of a single patient with HTN-induced PRES and Schwartz et al. (1992) reported transient increased perfusion on Tc99m-HMPAO SPECT in the regions of CT/MR abnormality in two patients with HTN-induced PRES. However, using dynamic susceptibility contrast MR perfusion imaging in fifteen patients with PRES, Bartynski and Boardman (2008) demonstrated significantly reduced CBV in most regions of PRES imaging abnormality compared with a reference healthy cortex. Similarly, in retrospective assessment of contrast MR perfusion imaging in eight patients with PRES, Brubaker et al. (2005) observed a significant decrease in CBF and CBV values in all patients compared to healthy volunteers.

These inconsistent findings may be in part related to small sample sizes, differences in technique or timing of imaging, and/or differences in the underlying pathophysiologic mechanism related to the various etiologies that can lead to PRES. For instance, HTN was the most common etiology of PRES among our sample, whereas in the study by Bartynski and Boardman (2008) most patients developed PRES in the setting of a systemic condition such as transplant, infection, sepsis, shock, oreclampsia. As such, the pathophysiology of PRES may vary depending on the causative factor that leads to BBB injury either by hyper- or hypoperfusion or toxin/immune-mediated endothelial dysfunction. For example, in the setting of HTN, PRES may be secondary to failed autoregulation/dysregulation of CBF, whereas, in the setting of

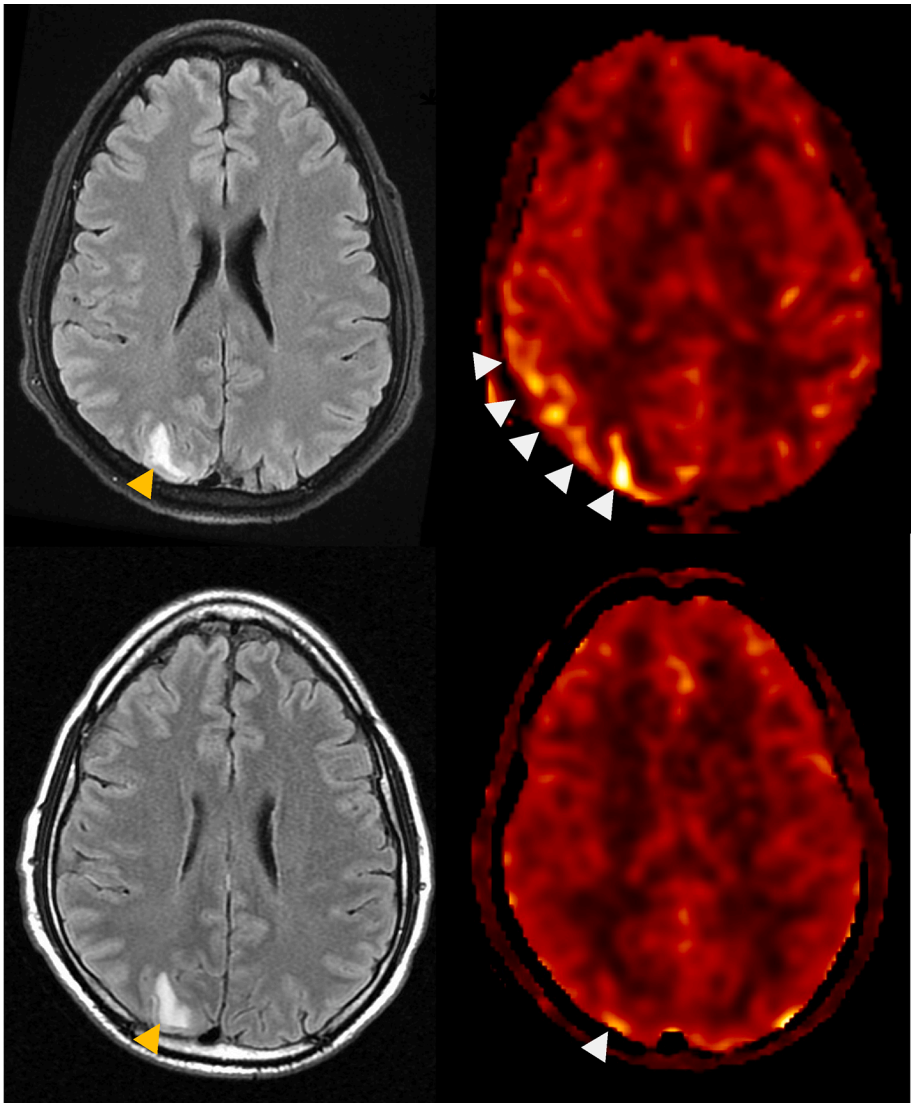

Fig. 5. Axial T2 FLAIR (left) and ASL color (right) perfusion maps on day 1 (top row) and day 3 (bottom row) of a 33-year-old male with methamphetamine-induced PRES. Hyperperfusion (white arrowheads) was near-completely resolved three days after the initial presentation while FLAIR hyperintensity (orange arrowheads) persisted. (For interpretation of the references to color in this figure legend, the reader is referred to the web version of this article.)

normotensive PRES, the mechanism may be based on endothelial dysfunction. Of note, the Bartynski et al. (Engelter et al., 1999) study that included fifteen patients was previously the largest study examining cerebral perfusion in PRES.

The time of imaging in relation to the onset of symptoms may have also influenced the result of perfusion studies. Whitlow et al. (2008) observed that PRES patients who were imaged acutely showed hyperperfusion, whereas those imaged in the subacute phase showed hypoperfusion. Similarly, in our study, patients who were imaged within 24 h of symptoms onset were more likely to show hyperperfusion on ASL compared to those who were imaged later during the course of the disease. In the one patient with available short-term follow up imaging (Fig. 5), we observed interval resolution of CBF changes, yet with persistent FLAIR signal abnormality three days after the initial presentation of PRES, which further supports the above theory. We also observed that CBF changes did not always exactly correspond to regions of vasogenic edema; in some cases, the vasogenic edema involved a much larger volume than the perfusion abnormality, whereas in other cases the converse was true. In one of our cases, vasogenic edema and perfusion abnormality were spatially distinct. These observations support the idea that perfusion changes and vasogenic edema may develop at different stages of the PRES continuum. In fact, the HTN-induced autoregulatory failure theory suggests that hyperperfusion precedes and ultimately leads to vasogenic edema; as such, it is plausible that regions of hyperperfusion without vasogenic edema simply reflect an early phase of disease, whereas regions with vasogenic edema but without perfusion abnormality are at a later phase of disease. Regions demonstrating both vasogenic edema and perfusion abnormality may reflect a more intermediate stage of disease. Inconsistent findings of PRES-associated perfusion changes across different studies may thus be at least partly related to temporal changes in cerebral perfusion associated with disease evolution. While we did not find a statistically significant association between ASL-FLAIR signal abnormality mismatch and time to imaging, this may have been due to the relatively small number of patients.

An interesting corollary to the above ideas is that early PRES may be underdiagnosed if MRI is obtained too early after symptom onset for vasogenic edema to develop. Moreover, since symptoms in PRES may resolve quickly (and with only minimal intervention such as lowering blood pressure), repeat imaging that would detect edema will often not be ordered. In this way, ASL-based perfusion could be used as a new biomarker for early PRES, independent of vasogenic edema.

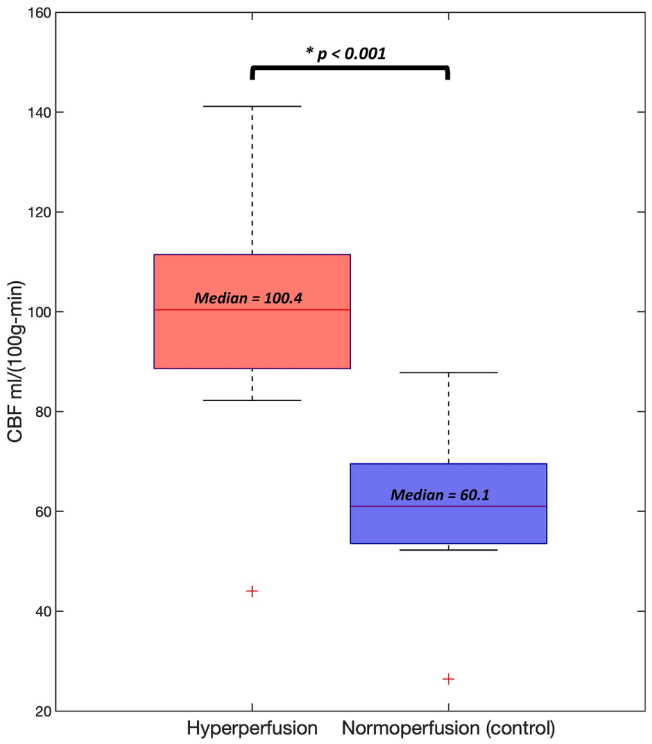

Fig. 6. Box-and-whisker plot of quantitative CBF in thirteen PRES patients with visually apparent hyperperfusion. CBF in regions of hyperperfusion relative to normal perfusion (control) is found statistically different at $p < 0.001$. Boxes depict interquartile range. Whiskers depict minimum and maximum values, excluding a paired outlier (plus signs).

Table 2
Demographic, clinical, and imaging covariates of Qualitative ASL perfusion.

	Overall	Hyperperfusion	Normal perfusion	P-value [1]
Number of patients, n (%)	20	13 (65%)	7 (35%)	
PRES etiology, n (%)				
HTN	13	9 (69.2%)	4 (30.8%)	0.65
Other	7	4 (57.1%)	3 (43.9%)	
MAP, median (IQR)	123 (107-147)	132 (10.8-154.5)	116 (103.5-134)	0.35
Age, median (IQR)	50.1 (32.8-59.7)	56.1 (32.8-61.5)	36.4 (28.6-53.1)	0.5
Gender, n (%)				
Female	11	9 (81.8%)	2 (18.2%)	0.33
Male	9	4 (55.5%)	5 (44.5%)	
Time to imaging, n (%)				
≤ 24 hours	14	12 (85.7%)	2 (14.3%)	**0.007** **
> 24 hours	6	1 (16.7%)	5 (83.3%)	
Restricted diffusion, n (%)				
No	13	9 (69.2%)	4 (30.8%)	0.61
Yes	7	4 (57.1%)	3 (42.9%)	
Microhemorrhage, n (%)				
No	12	7 (58.3%)	5 (41.7%)	0.64
Yes	8	6 (5%%)	2 (25%)	
Clinical/imaging outcome, n (%)				
Favorable	16	11 (68.7%)	5 (31.3%)	0.59
Unfavorable	4	2 (50%)	2 (50%)	

Notes: Row percentages are provided. IQR: interquartile range.
[1]P-values are calculated using Fisher's exact test for categorical variables and Wilcoxon Rank Sum test for continuous variables.
* <0.05 ** <0.01 *** <0.001.

An important feature of ASL, in contrast to DSC and CT perfusion, is its ability to quantify absolute CBF in well-established physiological units (ml/100 g tissue – min). Our quantitative analysis showed statistically significant CBF increases in PRES despite small sample size, suggesting that effect sizes are large for hyperperfusion, strengthening the value of ASL-CBF as a potential PRES imaging biomarker. The quantitative and easily repeatable nature of ASL-CBF also facilitates serial CBF monitoring in PRES. Thus, these factors could potentially alter ongoing management decisions (for example, treatment based on ASL hyperperfusion prior to the development/detection of the cerebral edema on FLAIR imaging).

Apart from the time of imaging in relation to symptom onset, no significant association was found between ASL perfusion and the remaining demographic, clinical, or imaging covariates.

The main limitations of our study include the small sample size and retrospective nature (i.e., all data had already been collected prior to the conception of this study). Despite this, our study comprises one of the largest patient cohorts among all studies of perfusion in PRES and because of the large observed hyperperfusion effect, our results are statistically significant even with a sample size of 20. However, additional associations between ASL perfusion and other parameters may be missed due to small numbers.

One notable confounder in ASL techniques is the so-called arterial transit artifact (ATA), which reflects elevated ASL signal residing in medium-large arteries rather that within the microvasculature/parenchyma. This can be erroneously interpreted as tissue hyperperfusion and result in a false positive. Thankfully, ATA has quite characteristic features; specifically, a distinct, often peripheral, curvilinear morphology that can localize to FLAIR hyperintensity within the sulci due to slow flow (i.e. the FLAIR 'ivy' sign). Conversely, true parenchymal hyperperfusion will be more homogeneous, less curvilinear, and not associate with an 'ivy' sign on FLAIR. Given the distinct appearance of ATA versus tissue and our multiyear experience with clinical ASL, we are quite confident that true hyperperfusion was properly identified in this study. ATA was seen in only one patient (confirmed by a positive 'ivy' sign) and not counted as hyperperfusion.

5. Conclusions

Our data support that ASL provides a practical way to identify and noninvasively monitor changes of cerebral perfusion in patients with PRES. The majority of PRES patients in this study demonstrated hyperperfusion on ASL, favoring failure of autoregulation as a predominant mechanism of PRES. In addition, hyperperfusion was more likely to be seen in patients imaged less than 24 h from symptoms onset, supporting the idea that perfusion changes and vasogenic edema may develop at different stages of the PRES continuum. ASL may thus provide information on the acuity of PRES and could potentially guide management strategies. Additional larger studies are needed to explore these ideas further and advance our knowledge of perfusion patterns in PRES physiology.

CRediT authorship contribution statement

Soudabeh Fazeli: Conceptualization, Methodology, Data curation, Formal analysis, Writing – original draft. **Abraham Noorbakhsh:** Methodology, Formal analysis, Writing – review & editing. **Steven G. Imbesi:** Conceptualization, Methodology, Supervision, Writing – review & editing. **Divya S. Bolar:** Conceptualization, Methodology, Data curation, Formal analysis, Supervision, Writing – review & editing.

References

Bartynski, W.S., 2008. Posterior reversible encephalopathy syndrome, Part 1: Fundamental imaging and clinical features. Am. J. Neuroradiol. 29 (6), 1036–1042.

Hinchey, J., Chaves, C., Appignani, B., Breen, J., Pao, L., Wang, A., Pessin, M.S., Lamy, C., Mas, J.-L., Caplan, L.R., 1996. A reversible posterior leukoencephalopathy syndrome. N. Engl. J. Med. 334 (8), 494–500.
Casey, S.O., Sampaio, R.C., Michel, E., et al., 2000. Posterior reversible encephalopathy syndrome: utility of fluid-attenuated inversion recovery mr imaging in the detection of cortical and subcortical lesions. Am. J. Neuroradiol. 21, 1199–1206.
Fischer, M., Schmutzhard, E., 2017. Posterior reversible encephalopathy syndrome. J. Neurol. 264 (8), 1608–1616.
Bartynski, W.S., 2008. Posterior reversible encephalopathy syndrome, Part 2: Controversies surrounding pathophysiology of vasogenic edema. Am. J. Neuroradiol. 29 (6), 1043–1049.
Schwartz, R.B., Bravo, S.M., Klufas, R.A., Hsu, L., Barnes, P.D., Robson, C.D., Antin, J.H., 1995. Cyclosporine neurotoxicity and its relationship to hypertensive encephalopathy: CT and MR findings in 16 cases. Am. J. Roentgenol. 165 (3), 627–631.
Anderson, R.-C., Patel, V., Sheikh-Bahaei, N., Liu, C.S.J., Rajamohan, A.G., Shiroishi, M. S., Kim, P.E., Go, J.L., Lerner, A., Acharya, J., 2020. Posterior Reversible Encephalopathy Syndrome (PRES): Pathophysiology and Neuro-Imaging. Front. Neurol. 11.
Feske, S., 2011. Posterior reversible encephalopathy syndrome: a review. Semin. Neurol. 31 (02), 202–215.
Marra, A., Vargas, M., Striano, P., Del Guercio, L., Buonanno, P., Servillo, G., 2014. Posterior reversible encephalopathy syndrome: The endothelial hypotheses. Med. Hypotheses 82 (5), 619–622.
Apollon, K.M., Robinson, J.N., Schwartz, R.B., Norwitz, E.R., 2000. Cortical blindness in severe preeclampsia: Computed tomography, magnetic resonance imaging, and single-photon-emission computed tomography findings. Obstet. Gynecol. 95 (Supplement), 1017–1019.
Hedna, V.S., Stead, L.G., Bidari, S., Patel, A., Gottipati, A., Favilla, C.G., Salardini, A., Khaku, A., Mora, D., Pandey, A., Patel, H., Waters, M.F., 2012. Posterior reversible encephalopathy syndrome (PRES) and CT perfusion changes. Int. J. Emerg. Med. 5 (1).
Wartenberg, K.E., Parra, A., 2006. CT and CT-perfusion findings of reversible leukoencephalopathy during triple-H therapy for symptomatic subarachnoid hemorrhage-related vasospasm. J. Neuroimaging 16, 170–175.
Vanacker, P., Matias, G., Hagmann, P., Michel, P., 2015. Cerebral Hypoperfusion in Posterior Reversible Encephalopathy Syndrome is Different from Transient Ischemic Attack on CT Perfusion. J. Neuroimaging 25 (4), 643–646.
Sarbu, N., López-Rueda, A., Chirife, O., Capurro, S., 2014. CT-perfusion time-maps likely disclose the earliest imaging signs of posterior reversible encephalopathy syndrome (PRES). J. Neuroradiol. 41 (2), 147–149.
Alsop, D.C., Detre, J.A., Golay, X., Günther, M., Hendrikse, J., Hernandez-Garcia, L., Lu, H., MacIntosh, B.J., Parkes, L.M., Smits, M., van Osch, M.J.P., Wang, D.J.J., Wong, E.C., Zaharchuk, G., 2015. Recommended implementation of arterial spin-labeled Perfusion MRI for clinical applications: A consensus of the ISMRM Perfusion Study group and the European consortium for ASL in dementia. Magn. Reson. Med. 73 (1), 102–116.
Whitlow, C., Pollock, J., Kraft, R., et al., Evolving Temporal Changes in Cerebral Blood Flow Associated with Posterior Reversible Encephalopathy Syndrome: A Magnetic Resonance Arterial Spin Labeling Investigation. In: American Society of Functional Neuroradiology. Orlando, Florida; 2008:217–8.
McKinney, A.M., Jagadeesan, B.D., Truwit, C.L., 2013. Central-variant posterior reversible encephalopathy syndrome: brainstem or basal ganglia involvement lacking cortical or subcortical cerebral edema. Am. J. Roentgenol. 201 (3), 631–638.
Schwartz, R.B., 2002. Hyperperfusion encephalopathies: hypertensive encephalopathy and related conditions. Neurologist 8 (1), 22–34.
Schwartz, R.B., Jones, K.M., Kalina, P., Bajakian, R.L., Mantello, M.T., Garada, B., Holman, B.L., 1992. Hypertensive encephalopathy: findings on CT, MR imaging, and SPECT imaging in 14 cases. Am. J. Roentgenol. 159 (2), 379–383.
Sanelli, P.C., Jacobs, M.A., Ougorets, I., Mifsud, M.J., 2005. Posterior reversible encephalopathy syndrome on computed tomography perfusion in a patient on “triple H” therapy. Neurocrit. Care 3 (1), 046–050.
Bartynski, W.S., Boardman, J.F., 2008. Catheter angiography, MR angiography, and MR perfusion in posterior reversible encephalopathy syndrome. AJNR Am. J. Neuroradiol. 29 (3), 447–455.
Brubaker, L.M., Smith, J.K., Lee, Y.Z., et al., 2005. Hemodynamic and permeability changes in posterior reversible encephalopathy syndrome measured by dynamic susceptibility perfusion-weighted MR imaging. Am. J. Neuroradiol. 26, 825–830.
Engelter, S.T., Petrella, J.R., Alberts, M.J., Provenzale, J.M., 1999. Assessment of cerebral microcirculation in a patient with hypertensive encephalopathy using MR perfusion imaging. Am. J. Roentgenol. 173 (6), 1491–1493.

Further reading

Amukotuwa, S.A., Yu, C., Zaharchuk, G., 2016. 3D Pseudocontinuous arterial spin labeling in routine clinical practice: a review of clinically significant artifacts. J. Magn. Reson. Imaging 43 (1), 11–27.